

Short Communication

A Non-aqueous Hybrid Supercapacitor with Porous Anatase TiO₂ Nanoparticles Anode and Activated Carbon Cathode

Dan Wang, Kai Xie, Yourong Wang, Siqing Cheng*

Innovation Center for Nanomaterials in Energy and Medicine (ICNEM), School of Chemical and Environmental Engineering, Wuhan Polytechnic University, Hubei 430023, P. R. China

*E-mail: icnem@hotmail.com

Received: 14 June 2016/ Accepted: 22 September 2016 / Published: 10 November 2016

The porous anatase TiO₂ nanoparticles were synthesized by a facile hydrothermal method and characterized by scanning electronic microscopy (SEM), transmission electronic microscopy (TEM) and powder X-ray diffraction (XRD). A non-aqueous hybrid supercapacitor with the as-prepared TiO₂ nanoparticles anode and activated carbon (AC, BP-2000) cathode was fabricated and investigated electrochemically. The results showed that the hybrid supercapacitor with the optimal mass ratio 1:2 of AC to TiO₂ delivers a specific capacitance of 48 F g⁻¹ at a current rate of 100 mA g⁻¹ and exhibits a good cycling stability. Within a voltage window of 0–3 V, 60.75 W h kg⁻¹ of energy is acquired at 150 W kg⁻¹, indicating the promising application of such hybrid supercapacitor in achieving both high energy density and power density to power the burgeoning hybrid electric vehicles (HEVs)/electric vehicles (EVs).

Keywords: Porous anatase TiO₂; Non-aqueous electrolyte; Hybrid supercapacitor; Electrochemical performance.

1. INTRODUCTION

Energy storage devices possessing both high energy density (batteries) and high power density (capacitors) have attracted intensive interest due to their wide range of applications from consumer electronics to traction devices.[1-3] Since Amatucci et al.[4] introduced the state-of-the-art concept of integrating lithium-ion batteries (LIBs) and capacitors, a novel energy storage device lithium ion capacitor (LIC) was proposed and burgeoned in the past decades, bridging the gap between high energy LIBs and high power capacitors.[3, 5-6] In principle, LIC is composed of a negative electrode of lithium ion battery coupled with a positive electrode of an electrochemical double layer capacitor (EDLC) immersed in a lithium-based non-aqueous electrolyte with an expanded voltage window, where the negative electrode works by lithium ion intercalation/deintercalation resulting in Faradaic

reaction, the positive electrode stores the charges via physical desorption/absorption and the electrolyte is usually a lithium salt (LiPF_6) dissolved in an organic solvent.[7-9] As such, the combination of the advantages of LIBs and capacitor opens a new avenue to effectively improve both energy and power density.

The major issue of constructing the LIC is to optimize suitable negative electrode material considering the kinetically sluggish Faradaic-intercalation reaction compared to non-Faradaic capacitive reaction of the positive electrode.[10-13] Thus, the negative electrode materials should necessitate high energy density, fast charging and/or discharging rates, long term cycling ability and less volume expansion during delithiation/lithiation.[14-16] Among various anode materials of lithium ion battery, anatase TiO_2 has been demonstrated to be promising negative electrode of LICs with capacitive nature because of its low potential, fast lithiation/delithiation, less distortion in structure during charge/discharge and long cycling lifespan.[17-21] Herein, we report the use of porous anatase TiO_2 as a negative electrode coupled with a activated carbon positive electrode in a LIC, with emphasis on the balancing of kinetics corresponding to the mass ratio between negative and positive electrode.

2. EXPERIMENTAL METHOD

2.1. Materials and synthesis

All used chemicals in this experiment were of analytical grade and purchased from Sinopharm Chemical reagent Co., Ltd, and used as received unless otherwise stated. A facile hydrothermal method was employed to synthesize the porous anatase TiO_2 using tetrabutyltitanate (TBT) as precursor. In a typical procedure, 5 ml of 30 wt% H_2O_2 was added into 50 ml single-neck flask containing 40 ml of distilled water under stirring, followed by the dropwise introduction of 1 ml of tetrabutyltitanate (TBT). After stirring for 10 min, 3 g of urea was added to form homogenous solution. Afterwards, the as-obtained solution was transferred into a 50 ml Teflon-lined stainless steel autoclave and heated at 170 °C for 2 h. After cooling to room temperature, the formed TiO_2 was collected by centrifugation and washed by ethanol and water for several times, and dried at 80 °C for 12 h. Finally, the as-obtained sample was annealed in a muffle furnace at 450 °C for 2 h to yield white powder product.

2.2. Structure characterization

Phase pure structure of the as-prepared porous anatase TiO_2 was characterized on a powder X-ray diffractometer (XRD) (Shimadzu DX-7000, Japan) using $\lambda = 0.154 \text{ nm}$ $\text{Cu K}\alpha$ radiation with 2θ degree from 10° to 70° at a scan rate of 4° min^{-1} . Scanning electronic microscopy (SEM, Hitachi) and Transmission electronic microscopy (TEM, JEOL TEM-2000) were used to characterize the morphology of the sample.

2.3. Electrochemical testing

Porous anatase TiO_2 electrodes were fabricated by blending the active material TiO_2 , conductive carbon black and binder polyvinylidene fluoride (PVdF) with the ratio of 8:1:1 in weight in N-methyl-2-pyrrolidone (NMP). The resulting slurries were evenly cast on Al foil as a collector and dried in a vacuum oven at 80 °C for 5 h and pressed for electrochemical testing. Likewise, the AC (BP-2000) electrodes were prepared by mixing different ratios of AC, conductive carbon black and binder PVdF in NMP in order to investigate the mass matching of positive to negative. Two-electrode cells were used for performance testing with polypropylene (Celgard 2400) as a separator, and 1 M solution of lithium hexafluorophosphate (LiPF_6) dissolved in the mixture of ethylene carbonate (EC) and dimethyl carbonate (DMC) (1:1 by mole) as a electrolyte. A half cell was assembled with metallic lithium as counter electrode while a full cell of hybrid supercapacitor with the as-obtained TiO_2 as negative electrode and AC as positive electrode in an Argon-filled Lab Mikrouna glove box. The cyclic voltammetry (CV) measurements were carried out on a CHI660B electrochemical workstation (Shanghai, China) and the galvanostatic charging-discharging tests were conducted on a LAND battery system.

3.RESULTS AND DISCUSSION

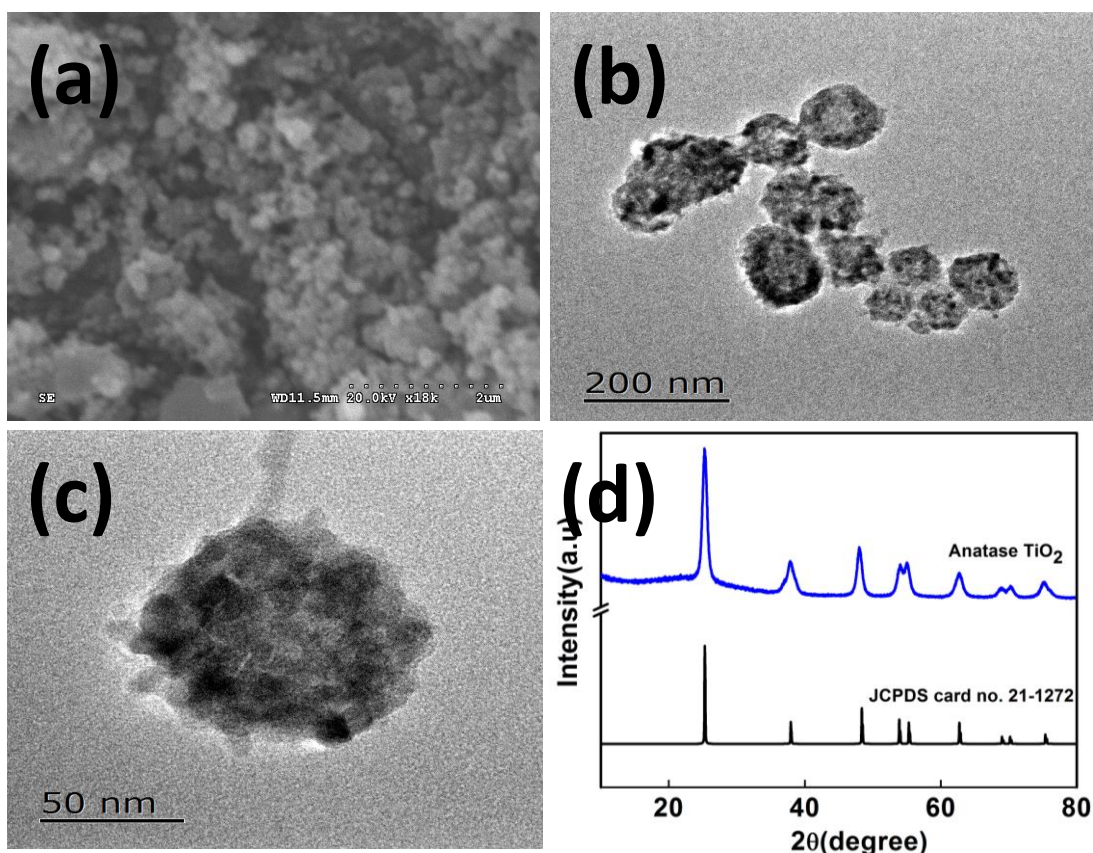


Figure 1. SEM image (a), TEM image (b), the magnified TEM image (c) and powder X-ray diffraction pattern (d) of the as-prepared TiO_2 .

The as-obtained almost evenly monodispersed porous TiO_2 nanoparticles with an average size of about 80 nm was fabricated by a facile hydrothermal approach using TBT as precursor, as shown in Fig 1a-c for the SEM and TEM images. Although many porous nanoparticles are seen vaguely from the SEM image in Fig. 1a, this is evident from the TEM image in Fig. 1b, and the magnified TEM image in Fig. 1c further reveals that the porous nano- TiO_2 is formed from the aggregation of tiny TiO_2 grains. As such, the crevices between tiny TiO_2 grains make up the porous structures, resulting in the multiporous TiO_2 nanoparticles with large specific surface area, which is suitable for capacitive or pseudocapacitive behavior when used as capacitor. The purity and crystal structure of the as-prepared porous TiO_2 nanoparticle was characterized by powder X-ray diffraction (XRD), as illustrated in Fig. 1d for the XRD pattern. The wide angle X-ray diffraction uncovers that the as-obtained multiporous TiO_2 nanoparticles are crystalline and the equivalent average grain size is about 4-5 nm according to the Scherrer's equation analysis [22] of the peak widths, which is consistent with the above results of TEM analysis. The identification of all X-ray diffraction peaks and their relative intensities could be indexed with the anatase TiO_2 phase without any impurities according to Joint Committee on Powder Diffraction Standards, JCPDS reference card no. 21-1272.

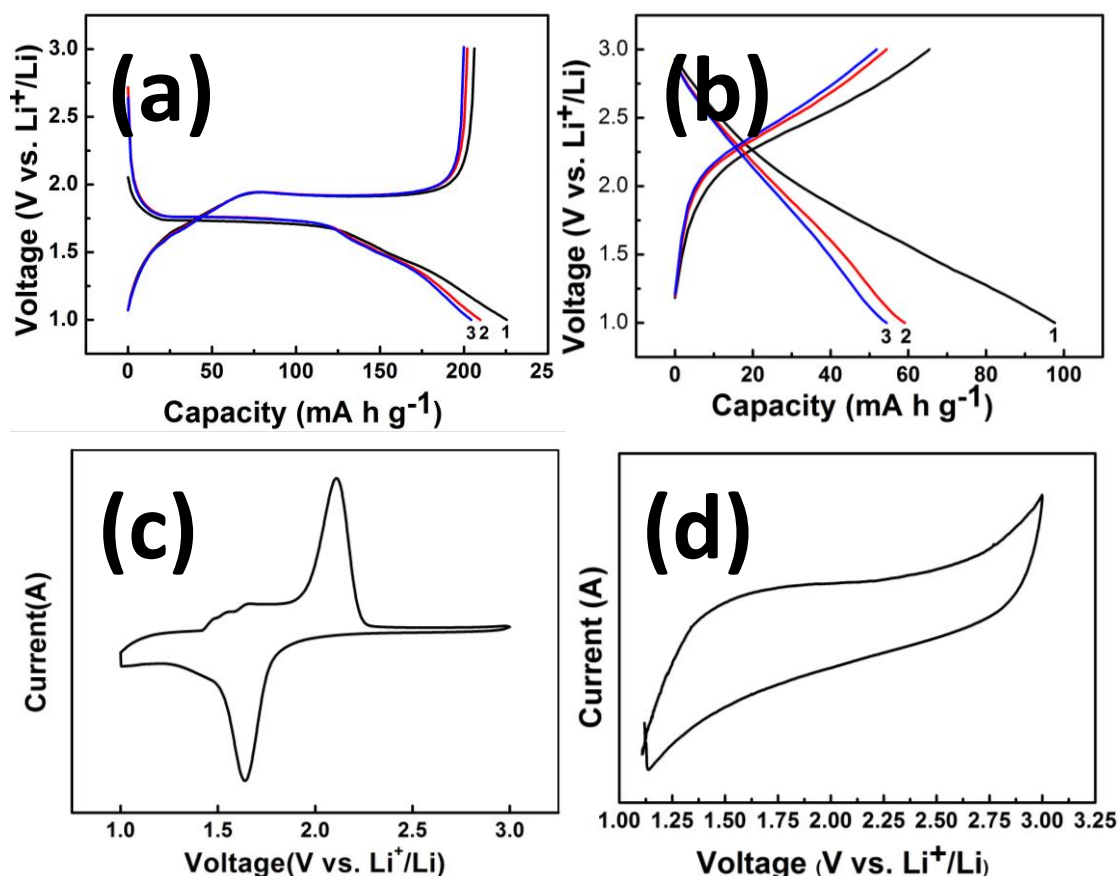


Figure 2. The galvanostatic charge/discharge profiles at a current rate of 100 mA g^{-1} and the cyclic voltammograms over the potential window of $1.0\text{-}3.0 \text{ V}$ at a scan rate of 1 mV s^{-1} of the TiO_2 electrode (a, c) and AC electrode (b,d).

Before exploring the hybrid supercapacitor with the as-prepared porous anatase TiO_2 anode and activated carbon cathode (BP-2000), the respective electrochemical properties of porous anatase TiO_2 and activated carbon (BP-2000) are investigated by constructing Li half-cells with metallic lithium as counter electrode, as shown in Fig. 2 for the galvanostatic charge/discharge curves at a current density of 100 mA g^{-1} in the voltage window of 1.0 to 3.0 V and cyclic voltammograms over the potential of 1-3 V at a scan rate of 0.2 mV s^{-1} . From Fig. 2a, it is seen that the charge/discharge behavior of porous anatase TiO_2 shows the characteristic voltage plateau corresponding to the oxidative/reductive peaks of cyclic voltammogram in Fig. 2c, indicating the reversible insertion of lithium into porous anatase TiO_2 nanoparticles. Also, the inappreciable discrepancy for the discharge capacities of the first three cycles is indicative of high reversibility of lithiation/delithiation of TiO_2 . However, the charge/discharge profiles of activated carbon (AC) are almost linear without any plateaus as shown in Fig. 2b, revealing the non-Faradaic capacitive operation mechanism of AC electrode via ionic adsorption/desorption on the surface, which correspond to the approximate rectangular cyclic voltammogram as shown in Fig. 2d.

In order to investigate the electrochemical performance of the as-obtained porous anatase TiO_2 nanoparticles in a non-aqueous hybrid supercapacitor, a full cell is constructed with porous anatase TiO_2 nanoparticles anode and AC cathode using a non-aqueous electrolyte consisting of 1 M LiPF_6 in EC/DMC. Fig. 3a shows the cyclic voltammograms of the assembled hybrid supercapacitors with different active material mass ratio of TiO_2 to AC in a voltage window of 0-3 V at a scan rate of 0.2 mV s^{-1} . In shape, it is supposed to come from the approximate overlay of separate cyclic voltammograms of TiO_2 electrode and AC electrode[23], which is not the typical rectangular CV profile for an ideal symmetric supercapacitor due to the concurrent redox and capacitive reactions.[24] The specific capacitances of the as-made hybrid supercapacitor with different active material mass ratio of AC to TiO_2 are evaluated from the galvanostatic charge/discharge profiles at a current rate of 100 mA g^{-1} using the following equation[25]:

$$C_p = \frac{I\Delta t}{m\Delta V} \quad (1)$$

where C_p is the specific capacitance of hybrid supercapacitor in F g^{-1} , Δt is the discharge time in second, m is the mass of the active electrode material in g, ΔV is the voltage window. From Fig. 3b, the calculated specific capacitances of the as-made hybrid supercapacitors are 33.7, 37.4, 48.6, 33.9 F g^{-1} when the mass ratios of AC to TiO_2 are 1:0.5, 1:1, 1:2, 1:3, respectively. What's more, the cycling stability for 100 cycles of the hybrid supercapacitor with different mass ratio of AC to TiO_2 is demonstrated in Fig. 3c, manifesting the long cycling stability of the fabricated hybrid supercapacitor with the difference in specific capacitance due to different mass ratio of AC to TiO_2 . Obviously, when the mass ratio of TiO_2 to AC in the hybrid supercapacitor is 2:1, the specific capacitance of 48.6 F g^{-1} is the highest, indicating the suitable balance of kinetics between anode and cathode. As such, the corresponding energy density E and power density P may be calculated to be $60.75 \text{ W h kg}^{-1}$ and 150 W kg^{-1} , respectively, based on the following equations (2) and (3)[7] in which the parameters are defined as the same as Eqn.(1), which is higher in E than EDLC (electrochemical double layer capacitor) and in P than battery. Compared with the recently reported result of 42 W h kg^{-1} of energy density [23], the higher energy density is obtained obviously, indicating the potential ability of the investigated system to construct the supercapacitor.

$$E = \frac{1}{2} C_p \Delta V^2 \quad (2)$$

$$P = \frac{E}{\Delta t} \quad (3)$$

In order to further explore the energy storage process of hybrid supercapacitor, the cyclic voltammetry of the hybrid supercapacitor with the optimal 1:2 mass ratio of AC to TiO₂ were carried out over potential range of 0-3 V at different scan rate, as illustrated in Fig. 3d. It is showed that the oxidative peak becomes wider with increasing the scan rate, indicating the dominant pseudocapacitive lithium transport instead of lithium storage process. On contrary, the low scan rate favors lithium storage process, exhibiting the obvious sharp oxidative peak.[26]

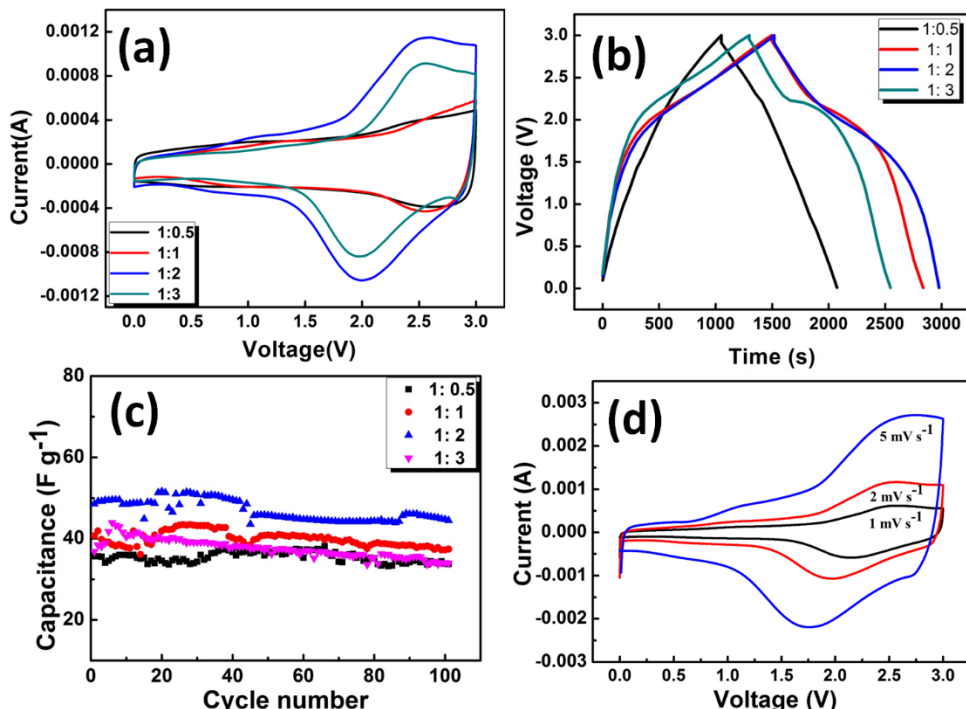


Figure 3. Electrochemical performance of the hybrid supercapacitor. (a) cyclic voltammograms with different mass ratio of AC to TiO₂ at a scan rate of 1 mV s⁻¹; (b) the galvanostatic charge/discharge profiles with different mass ratio of AC to TiO₂ at current density of 100 mA g⁻¹; (c) cycling stability for 100 cycles with different mass ratio of AC to TiO₂ at current density of 100 mA g⁻¹; (d) cyclic voltammograms with 1:2 mass ratio of AC to TiO₂ at different scan rate.

4.CONCLUSIONS

In summary, the multiporousanatase TiO₂ nanoparticles were fabricated successfully using a facile hydrothermal method with large specific surface area. The electrochemical measurements of separate TiO₂ and activated carbon (BP-2000) electrodes using lithium half-cells show the highly reversible lithiation of the as-prepared TiO₂ and the obvious capacitive properties via ionic adsorption/desorption on the surface. As such, the non-aqueous hybrid supercapacitor with porous

anatase TiO₂ nanoparticles anode and AC cathode is optimized with high specific capacitance of 48.6 F g⁻¹ when the mass ratio of AC to TiO₂ is 1:2, yielding 60.75 W h kg⁻¹ of energy at 150 W kg⁻¹ of power over the potential window of 0-3 V. Therefore, the proposed hybrid supercapacitor could sustain both high energy and power density, exhibiting the potential in powering the emerging hybrid electric vehicles (HEVs) and electric vehicles (EVs).

ACKNOWLEDGEMENTS

This work was supported by Hubei Provincial Natural Science Foundation of China (No. 2015CFC842), Education Science Foundation of Hubei Province (No. T200908), Project of Chinese Ministry of Education (No. 208088).

References

1. P. G. Bruce, S. A. Freunberger, L. J. Hardwick and J. M. Tarascon, *Nat. Mater.*, 11(2012)19.
2. E. J. Cairns and P. Albertus, *Annu. Rev. Chem. Biomol.*, 1(2010)299.
3. D. P. Dubal, O. Ayyad, V. Ruiz and P. Gomez-Romero, *Chem. Soc. Rev.*, 44(2015)1777.
4. G. G. Amatucci, F. Badway, A. Du Pasquier and T. Zheng, *J. Electrochem. Soc.*, 148(2001)A930.
5. A. D. Pasquier, I. Plitz, J. Gural, F. Badway and G. G. Amatucci, *J. Power Sources*, 136(2004)160.
6. F. Wang, S. Xiao, Y. Hou, C. Hu, L. Liu and Y. Wu, *RSC Adv.*, 3(2013)13059.
7. R. Kötz and M. Carlen, *Electrochim. Acta*, 45(2000)2483.
8. G. Wang, L. Zhang and J. Zhang, *Chem. Soc. Rev.*, 41(2012)797.
9. A. Yuan and Q. Zhang, *Electrochim. Commun.*, 8(2006)1173.
10. L. Gao, D. Huang, Y. Shen and M. Wang, *J. Mater. Chem. A*, 3(2015)23570.
11. Q. Ke, Y. Liao, S. Yao, L. Song and X. Xiong, *J. Mater. Sci.*, 51(2015)2008.
12. R. Liu, W. Guo, B. Sun, J. Pang, M. Pei and G. Zhou, *Electrochim. Acta*, 156(2015)274.
13. J. Wang, G. Yang, W. Lyu and W. Yan, *J. Alloys Compd.*, 659(2016)138.
14. Y.-G. Wang, Z.-D. Wang and Y.-Y. Xia, *Electrochim. Acta*, 50(2005)5641.
15. Y.-g. Wang and Y.-y. Xia, *Electrochim. Commun.*, 7(2005)1138.
16. Z. Zhong, Y. Yin, B. Gates and Y. Xia, *Adv. Mater.*, 12(2000)206.
17. T. Brezesinski, J. Wang, J. Polleux, B. Dunn and S. H. Tolbert, *J. Am. Chem. Soc.*, 131(2009)1802.
18. T. Brousse, R. Marchand, P.-L. Taberna and P. Simon, *J. Power Sources*, 158(2006)571.
19. A. G. Dylla, G. Henkelman and K. J. Stevenson, *Acc. Chem. Res.*, 46(2013)1104.
20. Z. Gao, Z. Cui, S. Zhu, Y. Liang, Z. Li and X. Yang, *J. Power Sources*, 283(2015)397.
21. Q. Wang, Z. H. Wen and J. H. Li, *Adv. Funct. Mater.*, 16(2006)2141.
22. M. Anis-ur-Rehman, A. S. Saleemi and A. Abdullah, *J. Alloys Compd.*, 579(2013)450.
23. H. Kim, M.-Y. Cho, M.-H. Kim, K.-Y. Park, H. Gwon, Y. Lee, K. C. Roh and K. Kang, *Adv. Energ. Mater.*, 3(2013)1500.
24. H. Tang, M. Xiong, D. Qu, D. Liu, Z. Zhang, Z. Xie, X. Wei, W. Tu and D. Qu, *Nano Energy*, 15(2015)75.
25. H. Zhou, X. Zou and Y. Zhang, *Electrochim. Acta*, 192(2016)259.
26. H. Liu, Z. Bi, X. Sun, R. R. Unocic, M. P. Paranthaman, S. Dai and G. M. Brown, *Adv. Mater.*, 23(2011)3450.